Annu. Rev. Astron. Astrophys. 1990. 28: 37–70

INTERSTELLAR DUST AND EXTINCTION

John S. Mathis

Washburn Observatory, University of Wisconsin-Madison,
475 North Charter Street, Madison, Wisconsin 53706

KEY WORDS: interstellar medium, molecular clouds, interstellar grains

1. INTRODUCTION

Interstellar dust is an important constituent of the Galaxy. It obscures all but the relatively nearby regions at visual and ultraviolet (UV) wavelengths and reradiates the absorbed energy in the far-infrared part of the spectrum, thereby providing a major part ($\sim$30%) of the total luminosity of the Galaxy. The far-infrared radiation from dust removes the gravitational energy of collapsing clouds, allowing star formation to occur. Dust is crucial for interstellar chemistry, in that it reduces the UV radiation, which causes molecular dissociations, and provides the site for the formation of the most abundant interstellar molecule, H_2. Probably grain surfaces are responsible for other chemistry as well. Dust controls the temperature of the interstellar medium (ISM) by accounting for most of the elements that provide cooling, as well as by providing heating through electrons ejected photoelectrically from grains.

The past decade has seen an increase in interest in interstellar dust because of the discovery of spectroscopic features in both emission and absorption, along with laboratory studies of candidate materials. There have been good observations of the extinction law of dust in many directions. Probably the most important feature to emerge from these studies is that "interstellar dust" refers to a variety of materials of widely varying properties.

Many studies of interstellar dust have involved lines of sight through the diffuse, low-density ISM, including some clouds having densities of up to several hundred H atoms per cubic centimeter. This material is referred

0066–4146/90/0915–0037$02.00

to herein as *diffuse dust*. In the literature, most references to "interstellar dust" apply to diffuse dust. Dust in the outer parts of molecular clouds that can be studied by optical and UV observations is called *outer-cloud dust*. Finally, there have been many studies of sources embedded so deeply within molecular clouds that only the near-infrared or perhaps optical part of the spectrum can be studied. This type of dust is referred to as *inner-cloud dust*. There is, of course, a continuous gradation of properties from diffuse dust to inner-cloud dust, but these three designations allow us to emphasize the rather different properties of interstellar dust in the various regions. This review is confined to diffuse dust and outer-cloud dust; for excellent reviews of inner-cloud dust, see (156, 157, 165).

Recent general references regarding interstellar dust are the proceedings of (*a*) a 1985 workshop held at Wye, Maryland (123); (*b*) the 1987 conference on "Dust in the Universe," held in Manchester, England (7); and (*c*) IAU Symposium No. 135 on "Interstellar Dust," held in Santa Clara, California, in July, 1988 (3). In general, reviews in these volumes on specialized aspects are not referenced here specifically. In addition, recent references are generally given in preference to older but important papers.

Extinction (absorption plus scattering) is by far the best-studied property of diffuse dust and outer-cloud dust because it can be determined accurately over a wide range of wavelengths and for lines of sight sampling different physical conditions in the ISM. Both continuous extinction and certain spectral features (narrow-wavelength regions over which the extinction varies appreciably) are discussed in Section 2. Another very important diagnostic is the emission from dust (Section 3), both in spectral features (which provide clues as to specific materials) and in the far-infrared (representing the emission from grains warmed by incident radiation or particles). Scattering (Section 4), polarization (Section 5), and other diagnostics (Section 6) also provide information. The evolution of dust is outlined in Section 7, and theories are discussed in Section 8. A summary is given in Section 9.

In this article I refer to the wavelength region $0.9\ \mu\text{m} < \lambda < 10\ \mu\text{m}$ as the near-infrared (NIR), $10\ \mu\text{m} \leq \lambda \leq 30\ \mu\text{m}$ as the mid-infrared (MIR), and $\lambda > 30\ \mu\text{m}$ as the far-infrared (FIR).

2. INTERSTELLAR EXTINCTION

2.1 *Continuous Extinction*

Each line of sight has its own "extinction law," or variation of extinction with wavelength, usually expressed by $A(\lambda)/A(V)$ in this article. This means of expressing the extinction law is not unique; it has been common practice to use instead the ratios of two colors, $E(\lambda-V)/E(B-V)$, where

$E(\lambda-V) = A(\lambda)-A(V)$. The use of $A(V)$ as the reference extinction is arbitrary, and it might be preferable to use instead a longer wavelength, such as the J bandpass (≈ 1.25 μm), because the extinction law would then be virtually independent of the line of sight (see Section 2.1.3). The information content of the extinction law is independent of how the law is expressed, but certain relations (see Section 2.1.1) become more obvious when $A(\lambda)/A(V)$ is used in place of $E(\lambda-V)/E(B-V)$.

2.1.1 OPTICAL/ULTRAVIOLET EXTINCTION OF DIFFUSE DUST AND OUTER-CLOUD DUST There have been several studies of the spatial distribution of extinction in the optical part of the spectrum (e.g. 51, 101, 122) that might be useful in estimating the amount of extinction in a particular direction, but this review concentrates instead upon the form of the extinction law and the physical nature of dust. Ardeberg & Virdefors (5) discuss the optical extinction law, with references.

Many authors have utilized the *International Ultraviolet Explorer* (*IUE*) to make detailed studies of the UV extinction law of diffuse dust and outer-cloud dust. There are considerable differences among the various lines of sight. Cardelli, Clayton & Mathis [19, 20 (hereinafter CCM89)] have used the UV observations of Fitzpatrick & Massa [54 (hereinafter FM86), 55, 109], with optical/NMR observations of the same stars, to explore the relationships between various extinction laws over the entire available interval of wavelengths. These observations were spread over the sky and included both diffuse dust and lines of sight to the Ophiuchus, Orion, and other molecular clouds, as well as to H II regions. CCM89 used the optical total-to-selective extinction ratio $R_V = A(V)/E(B-V)$ as a parameter. (R_V is determined by extrapolating NIR extinction to infinite wavelength.) Figure 1 shows the observed extinction laws of many lines of sight, plotted against R_V^{-1}, for several values of λ ranging from the red to almost the limit of the *IUE* spacecraft (1200 Å). There are fairly tight linear relationships between $A(\lambda)/A(V)$ and R_V^{-1} in each case, including the UV wavelengths.

The value of R_V depends upon the environment along the line of sight. A direction through low-density ISM usually has a rather low value of R_V (about 3.1). Lines of sight penetrating into a dense cloud, such as the Ophiuchus or Taurus molecular clouds, usually show $4 < R_V < 6$. However, it is not possible to estimate R_V quantitatively from the environment of a line of sight; for example, the star VI Cyg 12 lies behind a dense cloud of dust but has an R_V of 3.1 (78a), a value appropriate for the diffuse ISM. As a further example, $R_V \approx 3.0$–3.5 in parts of the Taurus cloud (159).

CCM89 fitted the slopes of the various $A(\lambda)/A(V)$–R_V^{-1} relations, examples of which are shown in Figure 1, by an analytic formula that

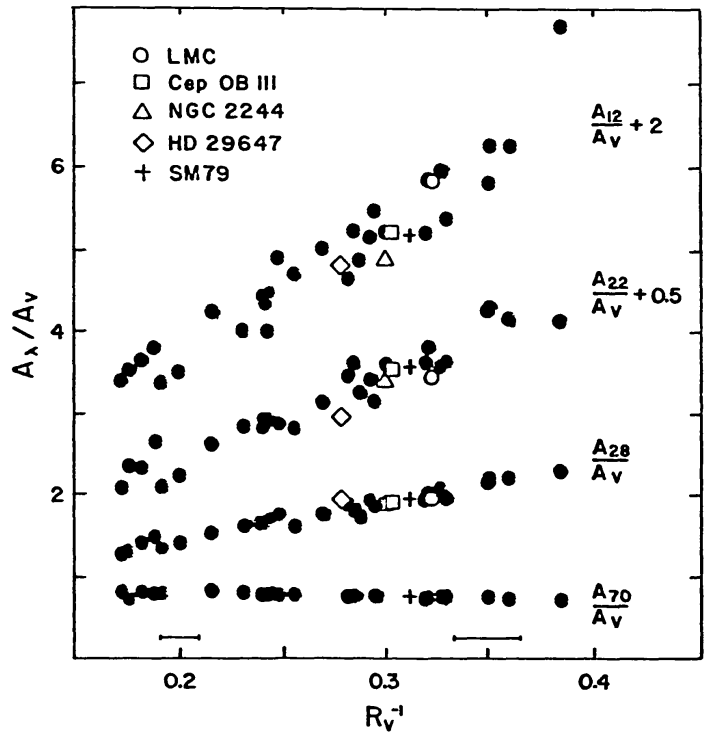

Figure 1 The observations of $A(\lambda)/A(V)$ plotted against R_V^{-1}, where $R_V = A(V)/E(B-V)$ (from CCM89). A_{12} refers to 1200 Å, A_{22} to 2175 Å, A_{28} to 2800 Å, and A_{70} to 7000 Å (the standard R filter). The black-dot observational values are from Fitzpatrick (53). The regularity of the observations and the scatter about the mean relationship are also shown.

represents the mean extinction law as a function of R_V. The expression is not reproduced here. Figure 2 (from CCM89) shows the mean extinction law for three values of R_V as calculated from the formula. Also shown are actual observations with the same values of R_V. The central curve is about as discrepant as actual observations are from the mean relationship. The dispersion of individual extinction laws around that mean law is shown in Figure 1 (from the spread in the individual observed points) and in the panel in Figure 2 (as error bars giving the standard deviation). The lowest set of curves plotted in Figure 2 are for Herschel 36, an exciting star of the H II region M8 and considered to have very "peculiar" extinction. Rather, Herschel 36 has a peculiar value of R_V (≈ 5.3) but a "normal" extinction law for that value of R_V. Note, however, that there are real deviations from the mean extinction law for any particular value of R_V. These deviations are especially large at 1200 Å, where the standard deviation of $A(\lambda)/A(V)$ from the mean extinction law is about 0.3. Extreme deviations might be found in the future and will provide valuable information regarding the processes that modify the grains.

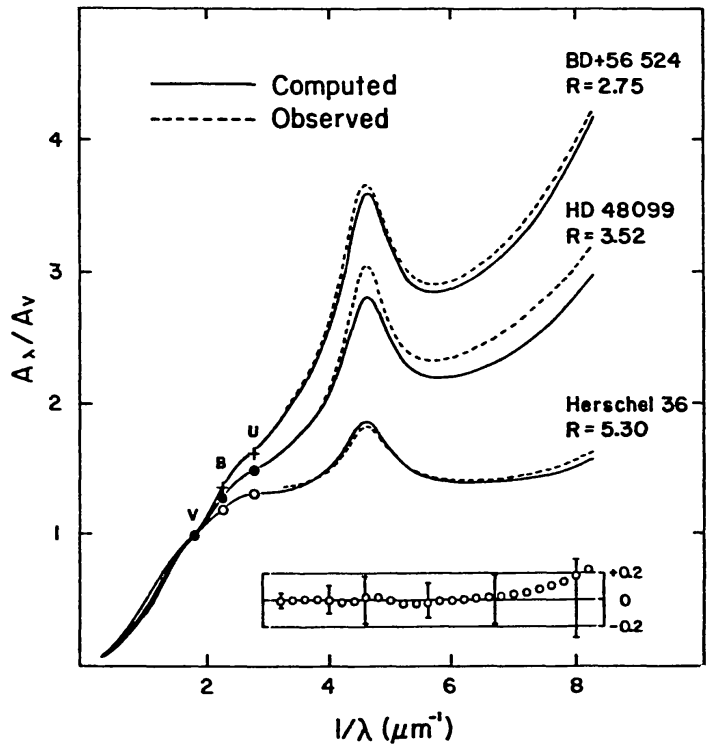

Figure 2 Three cases of a mean extinction law. Solid lines are obtained by fitting the slopes of the $A(\lambda)/A(V)$–R_V^{-1} relationship (Figure 1) by an analytic formula (CCM89), and dashed lines are actual extinction laws of stars (FM86) with the appropriate values of R_V. The error bars in the lower panel show the standard deviations of the observations of the entire sample (54) from the extinction law obtained from the formula. The open circles in the panel show the deviations from the "standard" mean extinction law (149) for the value $R_V = 3.2$, appropriate for the diffuse ISM.

The "mean" extinction laws of Savage & Mathis (144) and Seaton (149) are commonly used to correct observations for the presence of dust. Both laws are reproduced closely if $R_V = 3.2$ is substituted into the R_V-dependent mean extinction law given in CCM89. The panel in Figure 2 shows the deviations of the CCM89 mean extinction law, with $R_V = 3.2$ [from Seaton (149)]. It is not surprising that mean extinction laws correspond to an R_V slightly higher than 3.1; some lines of sight used in the averaging penetrate fairly dense regions.

Figure 1 shows that there is a continuous change between properties of diffuse dust, with $R_V \approx 3.1$, and outer-cloud dust, with large values of R_V. The two designations merely contrast one end of the observed range of R_V with the other.

The differences in the extinctions between diffuse dust and outer-cloud dust strongly affect any predictions concerning physical conditions inside

clouds. Figure 2 shows that outer-cloud extinction laws, i.e. those with $R \gtrsim 4$, rise much less steeply at shorter wavelengths than diffuse dust. Consequently, interstellar radiation incident upon a cloud can penetrate the cloud much more easily than would be predicted from the Seaton or Savage-Mathis extinction laws. Figure 3 shows the mean radiation intensity at the center of a cloud with a radial extinction of $A(V) = 5$ magnitudes (a typical value) computed using $R_V = 3.1$, and also with a typical outer-cloud dust value of $R_V = 5$. The difference in the predicted mean intensities has large implications for the physical processes in the cloud.

The fact that the extinction law depends so regularly on R_V suggests that the processes that modify the sizes and/or the compositions of grains must operate on all sizes simultaneously and quite efficiently. One could imagine that the small and large grains would be modified independently along various lines of sight, but such is not the case. The consequences of the regularity of the various extinction laws are considered in Section 7.

2.1.2 THE 2175-Å "BUMP" The strongest spectroscopic feature in the entire observed spectrum, in terms of equivalent width in frequency units, is the "bump" situated at 2175 Å, or 4.6 μm^{-1} (see Figure 2). The bump is present for all values of R_V. Its origin is not well understood (see ref. 38

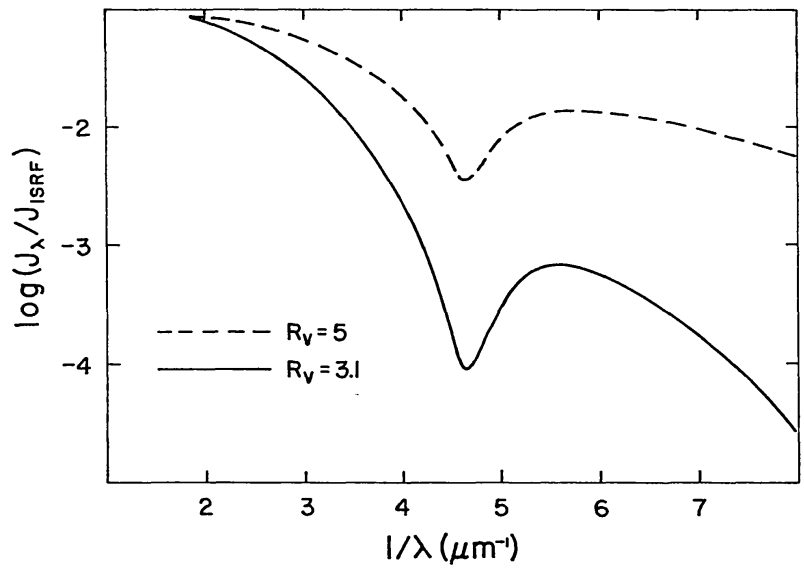

Figure 3 The mean intensity of radiation at the center of a cloud with a radial extinction of $A(V) = 5$ mag and no internal sources, expressed in terms of the mean intensity of the incident interstellar radiation field. Two values of $R_V[= A(V)/E(B-V)]$ are shown: one corresponding to the mean value for diffuse dust ($R_V = 3.1$), and the other for a typical observed value for lines of sight penetrating clouds ($R_V = 5$). The use of a mean extinction law corresponding to diffuse dust for predicting the radiation field within clouds leads to a gross error in the predicted radiation field within the cloud.

for an excellent review), although there is general (but not unanimous) agreement that it is probably caused by graphite or a slightly less well ordered form of carbon.

Let $A_{\rm bump}(\lambda^{-1})$ be the extinction at a wave number λ^{-1} between 3.3 and 6 $\mu{\rm m}^{-1}$ in excess of a linear extinction interpolated between the end points. The important properties of $A_{\rm bump}(\lambda^{-1})$ are as follows (176, FM86, CCM89):

1. The bump is extremely strong and must be produced by a very abundant material (which is why most theories attribute it to carbon). The equivalent width of the bump per $A(V)$, known from CCM89 or Seaton (149), can be expressed in terms of the oscillator strength, $f_{\rm bump}$, times the number of absorbing atoms, $N_{\rm bump}$. Bohlin et al (9) determined the mean $N({\rm H})/E(B-V)$, from which $N({\rm H})/A(V)$ follows. Dividing the expressions yields $N_{\rm bump}f_{\rm bump} = 9.3 \times 10^{-6}\, N({\rm H})$. Only the elements C, N, O, Ne, Mg, Si, and Fe (excluding noble gases) can provide enough absorption strength, even if the transition is exceedingly strong ($f_{\rm bump} \approx 1$). Each of the elements Fe, Si, and Mg require $f_{\rm bump} = 0.3$ even if the entire cosmic abundance is responsible for producing the bump, while 8% of the carbon would be required for the same $f_{\rm bump}$.

2. The central wave number λ_0^{-1} is surprisingly constant. For the stars in the FM86 sample, it is given by $\lambda_0^{-1} = 4.599 \pm 0.019$ $\mu{\rm m}^{-1}$, corresponding to $\lambda_0 = 2174 \pm 9$ Å. This amounts to a mean deviation of 0.4% in λ_0^{-1}, whereas other properties of the extinctions vary considerably. However, there are real variations in λ_0. The spreads of λ_0^{-1} for stars within a given cluster (101) are significantly less than among the field stars and serve to establish an upper limit to the observational errors. The stars HD 29647 and HD 62542 have especially peculiar extinctions (18), with $\lambda_0 = 2128$ Å and 2110 Å, respectively, that are smaller than the mean λ_0 by many standard deviations. These stars have the broadest bumps known (see below) but a rather small central absorption $A_{\rm bump}(\lambda_0)$, so that the integrated strengths of their bumps are about average. Their environments are very different, one being in a quiescent region in Taurus and the other in the Gum Nebula.

It is remarkable that graphite, a completely ordered and stable form of carbon, has a resonance very close to 2175 Å of about the right width and strength to produce the bump. Small graphite particles (radii < 0.005 μm) of various sizes and similar shapes would have the resonance at a common wavelength independent of size, but larger ones would have λ_0 shifted to longer wavelengths. Almost all theories suggest that the bump is produced by graphitic carbon in this way, along the lines suggested by Hecht (66).

3. The width of the bump, expressed as the full width at half-maximum

(FWHM), varies widely, currently with extremes of 0.768 μm^{-1} (HD 93028) and 1.62 μm^{-1} (HD 29647). The only significant correlation of the FWHM is with the mean gas density along the line of sight (FM86). The lack of correlation between the FWHM and λ_0^{-1} suggests that the variations in width are not caused by coatings of varying thicknesses upon a common carrier particle. Such coatings should produce a shift in λ_0^{-1} that is related to the change in width. This variation in width, unrelated to the position of the resonance, is difficult to explain with graphite of any size. The total area of the bump relative to $A(V)$, $\int A_{\text{bump}}(\lambda^{-1})/A(V)\, d\lambda^{-1}$, varies by over a factor of two among the FM86 stars.

4. The albedo of the bump probably has not been determined reliably. Lillie & Witt (98), using the observations of the diffuse galactic light from *Orbiting Astronomical Observatory 2*, suggested that the albedo drops across the bump. This is expected if the particles producing the bump are small (as suggested by the constancy of λ_0^{-1}, which can most easily be explained by absorption from small particles). However, plane-parallel axisymmetric geometry was used for interpreting the data, while the actual sky brightness in the UV is now considered to be uncertain and almost surely quite asymmetrical (see Section 6).

5. Two reflection nebulae show evidence of scattering in the bump, with a different profile in each (177), suggesting that some carriers of the bump can be large. (Small grains do not scatter.) This scattering is not observed in other nebulae. The expected shift in λ_0 to longer wavelengths (because of the relatively large particles causing the scattering) is not observed in the extinction of the exciting stars of these nebulae.

6. Observations of carbon stars (see Section 6.2) suggest that amorphous carbon, not graphite, is injected into the ISM. Perhaps *small* graphite particles can be produced later by annealing, but it is difficult to see how large graphite flakes can be made.

2.1.3 NIR CONTINUOUS EXTINCTION Figure 2 shows great differences in extinction laws among various lines of sight throughout the optical and UV portions of the spectrum. We might expect a corresponding variation at somewhat longer wavelengths, but apparently there is little if any.

Most NIR photometry is at the Johnson filters J (1.25 μm), H (1.65 μm), and K (2.2 μm). Whittet (166) tabulates $E(J-H)/E(H-K)$ as determined by several studies, in diffuse dust and outer-cloud dust alike, and finds them to be consistent with the value $E(J-H)/E(H-K) = 1.61 \pm 0.04$. Koornneef (87) considered a large body of data and suggests an extinction law that has a value of 1.70 for this ratio. Jones & Hyland (79) also concluded that NIR extinction is the same for both diffuse dust and outer-cloud dust, although they found $E(J-H)/E(H-K) =$

2.09 ± 0.10. The constancy of their ratio between lines of sight through diffuse dust and outer-cloud dust is more significant than the difference in the numerical value itself, which depends upon reduction to a standard photometric system.

The NIR extinction law is well fitted by the form $A(\lambda)/A(J) = (\lambda/1.25\ \mu\text{m})^{-\alpha}$. Recent values of α are 1.70 ± 0.08 (166), 1.61 (136), 1.75 (37), and ~ 1.8 (108). The value 1.70 seems a reasonable compromise for both diffuse dust and outer-cloud dust and implies that $E(J-H)/E(H-K) \sim 1.6$.

The constancy of the NIR extinction law implies that the size distributions of the largest particles are almost the same in all directions. This conclusion was also reached (111) on the basis of the interstellar polarization law, which involves only the largest particles.

2.1.4 FAR-UV EXTINCTION Martin & Rouleau (107) have extended the Draine & Lee (42; hereinafter DL84) opacities through the ionizing-UV range to X-ray energies (3.5 keV), assuming that grains are composed of silicates and graphite. The opacity rises to a maximum of 2.8×10^{-21} cm^2 (H atom)$^{-1}$ at 730 Å ($= 17$ eV) and declines to 7.4×10^{-22} cm^2 (H atom)$^{-1}$ at 124 Å ($= 100$ eV). At energies > 300 eV, the absorption law of the dust is approximately the same as if all of its atoms were neutral in the gas phase. At lower energies, especially just above the thresholds of abundant elements such as carbon, the large grains are opaque and the effective cross section per H atom is reduced. At 24 eV, the reduction amounts to a factor of four. The major effects of the dust as regards high-energy radiation are (*a*) to keep its constituents absorbing as neutral atoms, rather than possibly being ionized; and (*b*) to scatter the radiation, with a cross section about equal to the absorption cross section. This scattering can be observed as an X-ray halo around point sources (117). Dust does not affect the ionization equilibrium of H II regions very significantly (112) because its absorption, peaking at 17 eV, resembles hydrogen absorption too closely.

2.1.5 EXTRAGALACTIC EXTINCTION Reasonably reliable measurements for the extinction laws and dust/gas ratios exist only for the Magellanic Clouds. In the Large Magellanic Cloud (LMC), it is found that $R_V \approx 3.2 \pm 0.2$, virtually the galactic value (24, 86, 119). For the UV, the stars near the giant H II region 30 Doradus have weak bumps and extinctions rising steeply at the shortest *IUE* wavelengths, a behavior unfortunately known as "the LMC extinction law." However, the stars well away from 30 Dor (> 500 pc projected distance), spread throughout the Galaxy, have approximately galactic extinction laws (24, 53). The $N(\text{H})/E(B-V)$ is 2×10^{22} atoms mag^{-1} (53, 86), about four times the galactic value (9) and roughly proportional to the gaseous carbon abundance in the LMC.

In the Small Magellanic Cloud (SMC), there are almost no suitably reddened stars. In general there seems to be a low value of R_V, almost no bump, and a very steep far-UV rise (11, 121), as might be expected from a small R_V. One star, though, shows an extinction law similar to that of the Galaxy (96). The $N(\mathrm{H})/E(B-V)$ value is 4.6×10^{22} atoms mag^{-1}, about 10 times the galactic value and consistent with the gaseous C abundance in the SMC (104).

2.2 *The 9.7- and 18-μm Silicate Features*

Spectral absorption features can provide a great deal of information regarding the compositions and nature of the dust grains. Such features have not been detected in the UV (55, 148, 184), except, of course, for the bump. However, many have been found in the NIR, especially from the icy mantles within molecular clouds. In this review, we concentrate on diffuse-dust and outer-cloud dust and do not discuss the bands of molecular ices in general.

There is a broad, smooth absorption feature peaking at 9.7 μm, attributed to the Si–O stretch in silicates, which is always seen in interstellar dust if $A(V)$ is suitably large. The 9.7-μm band is found in emission from warm circumstellar dust surrounding oxygen-rich stars. In these objects the heavy elements (Fe, Mg, etc) are in silicates in the expanding envelope, while the carbon combines almost completely with oxygen to form CO. The 9.7-μm feature is not seen in circumstellar dust surrounding carbon-rich objects, except for some dusty planetary nebulae in which the grains were expelled by an earlier, and possibly oxygen-rich, phase of stellar evolution. A somewhat weaker and even broader feature peaking at 18 μm, the Si–O–Si bending mode, has been detected in circumstellar dust, in stars near the galactic center, and in molecular clouds (2, 118, 128, 160). The 18-μm band is much less well studied but is found with a strength relative to that of the 9.7-μm feature expected for silicates (about 0.4). The bands are polarized at the same angle (2, 84) with the amplitudes expected for silicates.

The strength and profile of the 9.7-μm band, relative to $A(V)$, have been determined (137) from several Wolf-Rayet type WC stars. These objects have the advantages of being luminous and of having no intrinsic spectral features in the 10-μm region (because they are carbon rich and therefore contain no circumstellar silicate dust). If $\tau_{9.7}$ is the optical depth of the silicate feature above the underlying continuum, the mean value of $A(V)/\tau_{9.7}$ in diffuse dust is 18.5 ± 1.0. However, there are substantial variations of $A(V)/\tau_{9.7}$ within the Taurus molecular cloud (169). The line of sight toward the galactic center has $A(V)/\tau_{9.7} \approx 9$, about half the local value (138), although the strong emission band at 7.7 μm confuses the

determination of the continuum underlying the band (28). The dust seems to be diffuse rather than in dense clouds; there are only weak radio lines from molecules commonly seen in molecular clouds. However, conditions in the inner Galaxy (chemical composition, for instance) certainly differ from those in our neighborhood.

The derived shape of the 9.7-μm band is uncertain because the band is only about half as strong at maximum as the continuous extinction at the K band (2.2 μm). In diffuse dust toward WC stars, the shape of the band is similar to the emission seen in dusty oxygen-rich stars such as μ Cep (99, 137). The emission profile near the Trapezium in the Orion Nebula is $\approx$40% broader (60) than in μ Cep, and the profile in dense clouds appears to be 10% narrower (128). It is not surprising that the shape of the band is different in various types of objects; very probably the silicates are in different states of order, with different degrees of impurities. I recommend the Roche & Aitken (137) profile as being typical of diffuse dust.

The 9.7-μm profile shows that interstellar silicate is not crystalline (16). Crystalline silicate absorption peaks at about 10.5 μm, rather than at 9.7 μm (see spectra in ref. 143). Laboratory measurements of amorphous or radiation-damaged silicates (33, 88) show a satisfactory, but not perfect, fit to the observed profile. Stars embedded in molecular clouds warm and partially anneal nearby grains (2).

The silicate band is weak for observational purposes, but it is difficult to account for its strength even if all of the silicon is in silicates and if a rather large opacity (3000 $cm^2\ g^{-1}$) is assumed for the maximum absorptivity (DL84, 157). This value is larger than most laboratory measurements of amorphous or lunar silicates. The total equivalent width of the band is rather constant from one type of silicate to another, so the broad profile of the interstellar band limits the maximum strength. The fundamental Kramers-Krönig relations (9a) limit the strength of the band (DL84) if astronomical silicates are similar to the minerals studied in the laboratory, but heavy contamination with other materials and perhaps a porous nature greatly complicate the issue.

There are suggestions that interstellar silicates are hydrated (68, 85), based on a 6.00-μm H–O–H bending band. However, in general the 6.00-μm feature is not correlated with the 9.7-μm band (172).

2.3 *Mean Extinction Laws*

Table 1 is an estimate of the extinction law for the observable range of wavelengths, normalized to J ($\approx$1.25 μm) because the extinction law is assumed to be independent of environment for $\lambda > 0.9$ μm. The reader can convert to $A(\lambda)/A(V)$ by means of the tabulated $A(V)/A(J)$ values. There are two columns for $\lambda < 0.9$ μm, representing the mean for diffuse

Table 1 Interstellar extinction and $A(\lambda)/A(J)$, where $J \approx 1.25$ μm[a]

λ (μm)	$A(\lambda)/A(J)$	λ (μm)	$A(\lambda)/A(J)$ $R_V = 3.1$	$A(\lambda)/A(J)$ $R_V = 5.0$	λ (μm)	$A(\lambda)/A(J)$ $R_V = 3.1$	$A(\lambda)/A(J)$ $R_V = 5.0$
250[b]	0.0015	5	0.095	0.095	0.24	9.03	5.13
100	0.0041	3.4	0.182	0.182	0.218	11.29	6.03
60	0.0071	2.2	0.382	0.382	0.20	10.08	5.32
35	0.013	1.65	0.624	0.624	0.18	8.93	4.66
25	0.048	1.25	1.00	1.00	0.15	9.44	4.57
20	0.075	0.9	1.70	1.70	0.13	11.09	4.89
18	0.083	0.7	2.66	2.43	0.12	12.71	5.32
15	0.053	0.55	3.55	3.06	0.091[c]	17.2	—
12	0.098	0.44	4.70	3.67	0.073	19.1	—
10	0.192	0.365	5.53	4.07	0.041	9.15	—
9.7	0.208	0.33	5.87	4.12	0.023	7.31	—
9.0	0.157	0.28	6.90	4.34	0.004	3.39	—
7	0.070	0.26	7.63	4.59	0.002	1.35	—

[a] $A(\lambda)/A(J)$ is the same for $\lambda > 0.9$ μm for all lines of sight, to within present errors. To estimate $A(\lambda)/N(\mathrm{H})$, multiply tabulated entry for $R_V = 3.1$ by 1.51×10^{-22} cm^2 (H atom)$^{-1}$. Except as noted below, entries are calculated from CCM89. Other values of R_V can be determined from that paper.

[b] For $\lambda > 250$ μm, multiply entry for 250 μm by $(250\ \mu\mathrm{m}/\lambda)^2$.

[c] For $\lambda < 0.1$ μm, entries are from (107), increased by 1.15 for continuity with the CCM89 extinction value at 0.12 μm.

dust ($R_V = 3.1$) and for outer-cloud dust ($R_V = 5$), both calculated from CCM89. The difference between the two laws is striking. The 9.7- and 18-μm feature profiles, as given by "astronomical silicate" (DL84), have been added to a power-law interpolation of an underlying continuum fitted between 250 and 7 μm. The profile of the silicate band was truncated at 25 μm, as is appropriate for circumstellar dust (128) but perhaps not for interstellar dust. The FIR opacity should be extrapolated to longer wavelengths with a λ^{-2} dependence (see Section 3.2.3); the value in the table is determined by the estimate of Hildebrand (70). The ionizing-UV cross sections are from Martin & Rouleau (107), adjusted by a factor of 1.15 to make them continuous with the extinction value of CCM89 at 0.12 μm. Both the "astronomical silicate" and ionizing-UV opacities are based upon the bare-silicate/graphite grain model (see Section 8) and depend (through the Kramers-Krönig relations) upon the assumption that interstellar grains have densities of ~ 3 g cm^{-3}.

The entries in Table 1 for $\lambda > 15$ μm are uncertain by at least a factor of two. There are as yet very few observational constraints upon the extinction law between the longer wavelengths of the silicate feature (which probably varies from one line of sight to another) and wavelengths $\lambda > 100$ μm, for which the energy is produced by steady-state emission from large

grains. The opacity at $\lambda > 100$ μm is somewhat constrained by the emission from isolated clouds warmed by the interstellar radiation field, which can be estimated.

3. EMISSION FROM DUST

3.1 *The Unidentified Infrared Bands*

The realization (150, 151) that diffuse dust produces strong unidentified infrared emission bands (UIBs) in the 3.3–11.3 μm range, as well as an associated continuum, has stimulated much research within the last five years. The carriers of the UIBs are surely important components of the ISM. The UIBs have been discussed extensively (3, 94, 133, 157), and some of their main features are the following:

1. The strongest bands are at 3.3, 6.2, 7.7, 8.6, and 11.3 μm. These wavelengths all closely correspond to the C–H or C–C bond vibrations in aromatic (benzene-ring) structures. The simplest substances that can produce these bands are simple, planar molecules called polycyclic aromatic hydrocarbons (PAHs), but other less well ordered configurations of carbon and hydrogen can also produce them (10, 142). A suggestive fit to the bands is provided by absorption from vitrinite (125), partially ordered graphite from coal. A mixture of PAHs can reproduce all of the UIBs, both weak and strong (57, 180).
2. Diffuse UIB emission, found throughout the Galaxy (59), is responsible for 10–20% of the total radiation from dust. UIBs and the associated continuum dominate the *Infrared Astronomical Satellite* (*IRAS*) filter responses at 12 and 25 μm (141), and are presumably responsible for the galactic "cirrus" emission seen with these filters (12).
3. The bands are also found in planetary nebulae, "reflection" nebulae, H II regions, extragalactic objects (27, 29, 171, and references therein), and carbon-rich or interstellar dust environments, *but not in dust produced by oxygen-rich objects*. There is a direct relationship between the C/O ratio in planetary nebulae and the strength of the UIBs (29).
4. The wavelength of the 11.3-μm UIB shows that the hydrocarbons are not saturated with H. This band is due to the out-of-plane C–H bending and occurs at 11.6–12.5 μm if there are two C–H bonds on the same aromatic ring, and at 12.4–13.3 μm for three bonds (94). The indicated amount of H coverage on the outer rings is 20–30%. Observational selection of relatively intense emission regions has meant that rather high radiation fields and subsequent dehydrogenation are favored; perhaps the 11–13 μm emission from low-radiation environments will indicate more than one C–H bond on the same ring.

5. The bands are excited by the absorption of a single UV photon by the carrier. This is easy to understand (133) if the carriers (planar PAHs or three-dimensional carbon structures no larger than about 5 Å) float freely in space, so that a single photon can provide the energy required to emit the UIBs. The degree of excitation suggests that roughly 50 carbon atoms are required, with an upward size range. If the carriers are attached to larger grains, the absorbed energy must be localized within a 5-Å region for the time required for the emission (of the order of a second). This process requires an *exceedingly* small thermal coupling.
6. The carriers of the UIBs are modified significantly by environment and history. The *IRAS* 12-μm response shows that the UIBs are not present in regions of very high radiation fields (13, 141), demonstrating that the carrier can be modified or destroyed by intense radiation. The wavelength of at least the 7.7-μm UIB is significantly different in planetary nebulae (where the carriers are newly produced by the carbon-rich material from the star) than in H II regions and reflection nebulae (where the carrier was presumably in the ISM before any interactions with the star presently causing the excitation).
7. PAHs would be mostly ionized in the diffuse ISM, since their first ionization potential is <13.6 eV. Up to now, many laboratory studies of PAHs have, necessarily, involved only neutral molecules.
8. An individual PAH has strong discrete absorption bands in the visual through the UV, *and there are no such features observed in interstellar extinction*. However, a mixture of PAHs of varying sizes and structural arrangements produces continuous absorption.

3.2 *Continuum Emission*

Continuum radiation from dust arises from two mechanisms: (*a*) fluorescence, giving rise to a red continuum; and (*b*) thermal radiation. The latter is observed either in the 1–60 μm range following the transient heating of a small grain by a single UV photon; or for $\lambda > 100$ μm, where the energy is reprocessed by steady-state emission of larger grains; or in the intermediate-wavelength range, where the effects compete.

3.2.1 RED CONTINUUM Grains in the "reflection" nebula NGC 2023 were found to produce a red continuum that peaks at about 6800 Å (178). Subsequent studies of many such nebulae confirm that there is an extended red emission in many of them (175, and references therein), typically contributing 30–50% of the flux in the *I* band (0.88 μm). In NGC 2023, the red emission is found in filamentary structures that spatially coincide with patches of H_2 infrared fluorescence and with the 3.3-μm UIB emission

(56) but not necessarily with the intensity of reflected light, which is determined by total dust density. IC 435, in the same molecular cloud, shows no red luminescence (174), nor does the Merope reflection nebula. A small patch of red fluorescent emission near the star γ Cas also shows a strong H_2 fluorescence in the UV (179). The "Red Rectangle" (HD 44179), a bipolar outflow excited by a central star, shows both strong UIBs and the red emission (140, 146).

The simplest interpretation of the red fluorescent emission is that it is excited by a strong UV flux incident upon hydrogenated carbon particles, either amorphous (46) or PAHs (32), thereby producing both the fluorescent red emission and the H_2 fluorescence. A strong enough radiation field will alter the carbon particles and dissociate the H_2, as might be the case in the Merope nebula.

3.2.2 3–30 μm CONTINUUM In addition to the UIBs, there is a continuous emission in the NIR/MIR range that accounts for a large part of the radiation from reflection nebulae (151) and, presumably, from the Galaxy as a whole. A survey at 11 and 20 μm (132) found unexpectedly high diffuse galactic emission. *IRAS* mapped almost the entire sky at 12, 25, 60, and 100 μm and found that the 12- and 25-μm intensities vary considerably relative to the 100-μm intensity (90, 91), which is roughly proportional to N(H I). The NIR/MIR emission arises from warm grains; simple considerations of the peak wavelength of the Planck function (and hence the emissivity of a grain) as a function of temperature show that this radiation must come from grains with temperatures of hundreds of Kelvins. By contrast, the mean local interstellar radiation field and optical constants for likely grain materials (carbon, silicates, organic refractory mantles) all suggest equilibrium temperatures of $\sim$20 K for the grains having the sizes ($>$0.01 μm) needed to account for the optical extinction (133). Grains of this size have large enough heat capacities so that their temperatures do not fluctuate appreciably after absorbing a single UV photon.

The NIR/MIR emission must be produced by grains in the size range 5–50 Å; such grains are large enough to have an almost continuous density of energy states. In this case they radiate a continuum rather than emission bands. A single UV photon heats the grain to a high peak temperature that depends upon the size of the grain and the energy of the photon (150). The grain emits the NIR/MIR radiation and cools to very low temperatures between photon absorptions. Calculations of thermal fluctuations (34, 41) have shown that very small grains can account for the spectrum of the emission. For clear discussions on the properties of small grains, see (4, 133).

3.2.3 FIR EMISSION Grains with sizes of 0.01 μm or more are cold

($\sim$20 K) and reradiate most of the energy that they absorb into the FIR part of the spectrum. Hildebrand (70) has clearly explained the process of determining grain properties and cloud masses from FIR observations. Cox & Mezger (30), in a recent review of the galactic FIR/submillimeter radiation from dust, estimate that about 10^{10} $L_{\odot}$, or 30% of the total luminosity of the Galaxy, is radiated in the FIR, mostly from dust heated in H I regions by the interstellar radiation field of early-type stars (12).

The FIR provides important information regarding the spatial variations of the interstellar radiation field throughout the Galaxy and on how molecular clouds form stars and evolve into H II regions, but it is of limited use as a diagnostic of dust because each line of sight samples grains with temperatures that depend upon their local radiation fields. However, for wavelengths much longer than about 150 μm (the peak of the emitted radiation), the FIR can be used to determine the relative opacities of the emitting grains. The Galaxy is optically thin at submillimeter wavelengths, in which case the intensity of emission I_λ is proportional to the opacity κ_λ times the Planck function $B_\lambda(T)$. For long wavelengths, $B_\lambda(T)$ varies linearly with the temperature, and thus the wavelength dependence of I_λ provides relative values of κ_λ. The results for diffuse radiation from the Galaxy (115) and from other galaxies (22) show that for $\lambda > 100$ μm, κ_λ is proportional to λ^{-2}, which is predicted by theory (e.g. DL84). The constant in the proportionality is difficult to determine because it depends on an estimation of the column density of grains, or of hydrogen, along the line of sight of the observation. The theoretical opacities of DL84, based on a graphite-silicate model for grains, are approximately half of Hildebrand's estimate (70) based on a calibration in local dense globules (cf 124). The uncertainties are probably at least a factor of two, if not more. Table 1 uses the Hildebrand value.

The mass of interstellar dust, and thereby an estimate for the mass of the ISM, is often determined from the FIR intensity, together with the opacity of grains per unit mass and an estimated grain temperature. It is important to realize (40) that this procedure is reasonably safe *only* if the observations are all on the long-wavelength side of the Planck function of the coldest grains—normally, in the submillimeter range. For instance, the "temperature" obtained from the ratio of the 60- and 100-μm intensities from *IRAS* is biased by a few warm grains that can provide almost all of the 60-μm emission. One can easily be off by a substantial factor (>3) in the resulting mass estimate!

In dust surrounding very young objects, bipolar outflows, or the cores of giant molecular clouds, the flux suggests that the opacity even in the submillimeter range (400–1300 μm) might vary as λ^{-1} or $\lambda^{-1.5}$ (145, 162, 181) instead of as λ^{-2}. The nebulae might be so optically thick that

radiative transfer effects are important at submillimeter wavelengths. However, the grains in these extremely dense objects might not be extremely small in comparison to 1 mm. Cometary grains also extend up to this size range. The growth of fractal grains (182; see Section 8) would explain the observations.

4. SCATTERING FROM DUST

Scattering from grains provides another diagnostic for their nature and composition, since cross sections for scattering at any angle (the "phase function") can be computed for a given material in much the same way as for extinction. However, the relative locations of the illuminating sources, the scattering grains, and the observer are very important in determining the actual intensity of scattered radiation. The presence of fluorescent emission (Section 3.2.1) complicates the interpretation of red and NIR scattering, but there seems to be little fluorescence in the range $\lambda < 0.5$ μm (139).

In practice, the geometry is so uncertain that one attempts to determine only two quantities characterizing the scattering process: the albedo, or the fraction of the extinction that is scattering; and g, the mean value of the cosine of the angle of scattering. For isotropic scattering, $g = 0$; for completely forward-throwing scattering, $g = 1$.

Scattering can be observed in three general situations: (*a*) the "diffuse galactic light" (DGL)—i.e. scattering by the diffuse dust of the general incident interstellar radiation field—which is strongly concentrated in the galactic plane, since the dust has a relatively small scale height; (*b*) reflection nebulae, with a known source of illumination (usually a B or A star because of their favorable luminosities); and (*c*) scattering of the general interstellar radiation field by a dark cloud, seen at high enough latitudes so that it contrasts with a relatively dark sky background.

The DGL in the optical part of the spectrum has been analyzed (110, 173). It is quite faint and asymmetric in its angular distribution and requires careful correction for the contribution of faint stars, airglow, and (especially) zodiacal light. Its advantage is that the geometry of the sources and scatterers is well known, in contrast to reflection nebulae. Witt (174) quotes a study (158) from *Pioneer 10* at 3 AU (so that both the airglow and zodiacal light are negligible) in which Toller (158) finds the albedo at 0.44 μm to be 0.61 ± 0.07 and g equal to 0.60 ± 0.22. Grains exhibit strong forward throwing scattering in the optical.

In the UV, there are surprising spatial fluctuations in the diffuse brightness of the sky, with background intensities ranging over an order of magnitude at the same wavelength (cf 77, 103, 120, 127, 155). The minimum

N(H I) presently observed in the sky corresponds to $A(V) \approx 0.05$ mag (100), or a scattering optical depth of ~ 0.06 at 0.16 μm. This translates into a sky brightness that is comparable to that observed. There may be an extragalactic component (which, in fact, is a common interpretation of the observed brightness). Clearly, the properties of grains or the intensity of any extragalactic component cannot be analyzed until the scattered intensity is known.

Reflection nebulae, in which a bright star illuminates a nearby scattering cloud, have been analyzed in some detail by various authors. Their advantages over the DGL and scattering by clouds are that they are much brighter, and that they are reflecting light from well-studied early-type stars, whereas the DGL and the clouds (discussed below) are illuminated by the much less well known interstellar radiation field (especially at UV wavelengths). Reflection nebulae suffer from three disadvantages: (*a*) The geometry of the star and scattering particles is not well known, and the placement of a given grain relative to the star and observer is crucial for determining how much light it scatters into the observer's line of sight. Simple geometries used in modeling the scattering, such as plane-parallel or spherical, are not so appropriate as one would like. (*b*) The patchiness of the dust is more serious for the reflection nebulae than for the DGL or the clouds. For clumpy objects, mean values of the albedo and g determined for the clump may not represent the values for a single scattering from an individual grain. (*c*) Some of the scattering is at large angles, in which case the assumed form of the phase function becomes important in the analysis. Astronomical observations of scattering have been interpreted by theoretical analyses employing the simple analytical Henyey-Greenstein (HG) phase function (69), which is computationally convenient but has no physical basis. The HG function is suitable for analyzing scattering at small to modest angles (<1 rad), in which case the important quantity is the fraction of the light thrown almost in the forward direction, but the HG function is not realistic for large-angle scattering.

Whether the advantages of reflection nebulae for determining the scattering properties of dust outweigh the disadvantages is a matter of opinion. I feel the geometrical uncertainties are such that results should be taken with considerable caution. Witt (174, and references therein) disagrees, arguing that the brightest reflection nebulae must have a common geometry in which the intensity of scattered light is maximized. He also points out that in the UV there might be three wavelengths at which the extinction optical depth is the same (two on each side of the bump and one in the steeply rising part of the extinction law at very short wavelengths; see Figure 2). In this case differences in the scattered light relative to the illuminating star's luminosity directly reflect changes in the grains' albedo.

His conclusion that g is smaller (more isotropic scattering) at $\lambda < 2000$ Å than for longer wavelengths seems correct.

Possibly small, relatively isolated interstellar clouds ("globules") contain dust that is more like outer-cloud dust than diffuse dust, but the determination of their optical properties is still of considerable interest. The geometry of scattering from globules at high enough latitude to be seen against a dark background (free from the DGL in the plane) is better known than for other reflection nebulae. At optical wavelengths, a cloud is seen strongly limb brightened from scattered radiation from behind (52), which is a direct indication of highly forward-throwing scattering by the grains in the optical. If the scattering were isotropic, the center of the cloud (with the greatest optical depth) would be brightest. Mattila (116) determined an albedo of ~ 0.6 and $g \approx 0.75$ by comparing the brightnesses of two globules at different latitudes and assuming that their dust is intrinsically similar.

5. POLARIZATION

Interstellar polarization arises from the propagation of radiation through the ISM containing aligned, elongated interstellar grains. The galactic magnetic field is responsible for aligning the grains (71), which spin with their long axes perpendicular to the field. Under these conditions, radiation is subjected to extinction, to linear dichroism (differential linear extinction for the two waves polarized along and perpendicular to the direction of alignment), and to linear birefringence (differential phase shift between the two waves). The birefringence produces circular polarization from the linearly polarized light, but the quantitative interpretation of the circular polarization to date has not been very fruitful because it depends upon the unknown geometry of the change of direction of grain alignment along the line of sight.

In principle, polarization is a diagnostic that provides another integral of a grain property over the size distribution, similar to extinction and scattering. However, it involves an additional function that is poorly understood: the alignment of grains of various sizes (reviewed in ref. 71). Even so, polarization is important because it provides information regarding the optical properties of grains and the conditions under which grains can be aligned.

5.1 *Continuum Polarization*

5.1.1 OPTICAL AND NIR The empirical wavelength dependence of optical/NIR polarization (151a) follows "Serkowski's law," i.e. $p(\lambda)/p(\lambda_{max}) = \exp[-K\ln^2(\lambda/\lambda_{max})]$, where λ_{max} is the wavelength of the maxi-

mum polarization $p(\lambda_{max})$. The quantity K was originally taken to be 1.15, but an improved fit (170) is $K = -0.10 + 1.86\lambda_{max}$. This law is entirely empirical, and it would be important to determine deviations at large $|\ln(\lambda/\lambda_{max})|$. Salient features of the optical polarization law are the following:

1. The averaged value of λ_{max} is 0.55 μm (151a), with extremes from about 0.34 to about 1 μm. The values of λ_{max}, determined by a least-squares fitting to Serkowski's law rather than a direct search for the maximum, depend mainly upon the observations at extreme wavelengths.
2. The polarization typically rises with wavelength through the ground-based UV to a maximum in the optical and then falling slowly through the NIR. Such behavior bears little resemblance to the extinction law, which keeps rising monotonically, except for the bump, toward shorter wavelengths throughout the observable UV. The grains responsible for the extinction in the ground-based UV do not participate in polarization because they are not elongated and/or not aligned.
3. The value of λ_{max} is almost proportional to R_V (25, 167, 168), although there is more scatter in the relationship than for the extinction laws. To a large extent, optical polarization measurements can substitute for NIR extinction in obtaining R_V.
4. The polarization law $p(\lambda)$ varies as $p(\lambda) \propto \lambda^{-1.8}$ for both diffuse dust and outer-cloud dust in the range 0.9 μm $< \lambda <$ 5 μm (108). The polarization law exponent is less well determined than for extinction, varying between -1.5 and -2.0 for various samples, but it is certainly similar to the value for extinction (-1.7--1.8; see Section 2.1.3). Note that this relation involves the absolute polarization, not relative to $p(\lambda_{max})$. The optical $p(\lambda)$ does vary strongly with R_V (see point 2 above), and the silicate feature has strong polarization that dominates for $\lambda > 5$ μm. The independence of $p(\lambda)$ from R_V again suggests that the size distribution of large grains is similar for clouds and the diffuse ISM.
5. The maximum value of $p(\lambda_{max})/A(\lambda_{max})$ is about 0.03 mag^{-1}, far less than from perfectly aligned spinning cylinders [0.22 mag^{-1} (111)]. This is interesting because the polarization direction closely follows the contours of the edges of several molecular clouds, presumably in regions where hydrogen changes its state from molecular to atomic relatively abruptly in space and perhaps in time. If the alignment mechanism keeps grains aligned under these adverse conditions, one would expect almost complete alignment when conditions are favorable, and a larger value of $p(\lambda_{max})/A(\lambda_{max})$ than is observed, in directions where the line of sight is perpendicular to the field. Perhaps there are two or more separate types of grains, only some of which are aligned. Alternatively, all grains might be

well aligned but have shapes that are less efficient than a spinning cylinder for producing polarization. A third possibility is that there is always a randomly oriented component to the field.

6. Polarization in the UV is unknown except for two stars (58). These limited data suggest that the bump is unpolarized. Upcoming observations from space (the WUPPE experiment on ASTRO missions) should provide many data. The polarization of the $\lambda 2175$ bump has been predicted if the bump is produced by aligned graphite (36).

An explanation for the form of the polarization law (111) assumes that grains can be aligned only if they contain one or more "superparamagnetic" particles (magnetite or other magnetic materials), which dissipate rotational energy as heat. Large grains are preferentially aligned because they are relatively likely to contain inclusions. Polarization is not specific to any particular grain model; if the large grains are aligned and a model predicts the extinction correctly, it will do well for the polarization also.

5.1.2 FIR POLARIZATION Polarization is observed in the emission from grains deep within the Orion Molecular Cloud and Sgr A, near the galactic center (35, 72, 163). The direction of the FIR polarization is perpendicular to the optical, exactly as expected: Light transmitted in the optical is polarized in the direction of smaller absorption. Emission, on the other hand, is largest in the direction of largest absorption.

Grain alignment is even more difficult for dense clouds than for the diffuse ISM (71). Alignment depends upon the grain being far from equilibrium with its surroundings, in which case there is no preferred axis because of the equipartition of energy. Deep inside a cloud, a grain should come to thermal equilibrium with the dense surrounding gas. The fact that polarization is observed shows that the rotation of aligned grains within clouds is not thermalized; they are presumably kept spinning in a particular direction because of the ejection of particles (H_2 after formation, or electrons) from particular sites (134), so the momentum of the ejected particles is not random. However, deep inside a cloud one would expect the gas impinging upon the grain to already be overwhelmingly H_2. Probably there also needs to be an enhanced dissipation of energy by superparamagnetic inclusions in the grains.

5.2 *Polarization in Spectral Features*

Inner-cloud dust provides information about diffuse dust through the polarization in the 3.08-μm ice band and the 9.7- and 18-μm silicate bands. If the polarization arises from aligned grains, the profiles of polarization, as compared with the corresponding extinction, are potentially important

diagnostics for both the shapes and the types of grains (DL84, 105). If the sizes and optical properties of interstellar grains are such that the light wave acts as a uniform electromagnetic field across the particle (the "Rayleigh approximation"), the extinction and polarization cross sections are both simple functions of the optical constants of the material. The Kramers-Krönig relations force a relationship between the optical constants and, therefore, the extinction and polarization. When there is a strong frequency variation of the optical constants, as across a spectral band, the polarization peaks at longer wavelengths than does the extinction. Indeed, the silicate polarization peaks at about 10.5 μm, whereas the extinction peak is at 9.7 μm (1, 2). The amount of shift depends upon the shapes of the grains as well as upon the optical constants. If the band is strong enough, there is a polarization reversal at wavelengths on the short side of the maximum polarization. The presence of coatings also affects the shape of the polarization relative to the extinction, even if the coatings have a weak wavelength dependence of optical constants across the band.

Polarization can be produced by scattering in the NIR as well as by extinction due to aligned grains. Such scattering, commonly observed in reflection nebulae around sources in dense, star-forming regions (95, 129, 130), shows that grains in very dense regions have grown to sizes of at least the order of 1 μm, partly by acquiring the ice coatings producing the 3.08-μm band.

In the Becklin-Neugebauer (BN) object in Orion (see ref. 93 for references), the linear polarization is strong (16%) in the 3.08-μm ice band, as opposed to $\sim 10\%$ in the neighboring continuum. The polarization is $\sim 15\%$ in the 9.7-μm silicate feature but only $\sim 1\%$ in the continuum. The position angle is constant across the bands and is the same as in the nebula in general, as expected from grain alignment but not from scattering. However, there is a reflection nebula around BN (see references in ref. 129) that complicates the interpretation of the polarization. By assuming that the polarization in BN is entirely from aligned grains, Lee & Draine (93) found grains are oblate (disk shaped) rather than prolate, with modest (2:1) axial ratios. One consequence of oblate grains is that the degree of alignment required is dropped by a factor of two, which is the ratio of the mean polarizing power of oblate and prolate grains.

A potentially powerful diagnostic for grains is the comparison of the polarizations in the 9.7- and 18-μm silicate bands, for which many of the geometrical uncertainties, such as angles of the magnetic field relative to the line of sight to the source, cancel because the same particles produce both bands.

6. OTHER DIAGNOSTICS OF INTERSTELLAR DUST

6.1 *Depletions in Interstellar Gas*

The strengths of the interstellar absorption lines of various ions in the spectra of background stars indicate the ionic column densities in the gas phase and, by inference, the amounts of the elements in grains. Jenkins (78) reviews the method of analysis, results, and several pitfalls. The principal results of depletions as regards grains are as follows:

1. The elements O, N, and Zn are only slightly depleted with respect to solar abundances, and their depletion does not vary measurably between dense and diffuse gas. The errors are such that these elements could be either undepleted or depleted by a factor of two.
2. Depletions of other elements increase significantly with average gas density along the line of sight. The elements P, Mg, and Cl are almost undepleted in diffuse gas ($\langle n(\mathrm{H})\rangle \approx 0.1$ cm^{-3}) and are depleted by about an order of magnitude when $\langle n(\mathrm{H})\rangle \approx 10$ cm^{-3}.
3. The elements Fe, Cr, and Si are depleted by about one order of magnitude in the diffuse ISM, and the depletions go roughly as the square root of the mean gas density, so that their depletion is about a factor of 10 more than P, Mg, and Cl, over a wide range in mean gas density (80). Thus, these depletions are two orders of magnitude along lines of sight through dense gas. This difference in depletion between outer-cloud dust and diffuse dust implies that grains evolve as they go from one environment to another. The elements Ca, Ti, and Al have similar depletions in low-density gas but a steeper dependence of depletion on mean gas density.
4. The depletion of C is, unfortunately, not reliably determined except for one line of sight: toward δ Sco with the *Copernicus* satellite (73). For observations with *IUE*, all lines of C^+, the dominant ionization stage in H I regions, lie on the "flat" (insensitive) portion of the curve of growth. For δ Sco, about 25% of the C is in the gas phase, which is about the amount found in CO in molecular clouds. The gas-phase carbon in the diffuse ISM is apparently simply converted to CO in molecular clouds, whereas the solid fraction remains approximately fixed.

There is some confusion in the literature because the C depletion can be *crudely* estimated from the well-determined gas-phase abundance of neutral C by estimating C^0/C^+. Unfortunately, the ionization corrections are factors of hundreds to thousands!

5. At a given mean gas density, there is a surprisingly small dispersion of the depletions (about ± 0.3 dex), whereas some depletions vary by one

or two orders of magnitude. Much of this dispersion must arise from averaging various local conditions along the line of sight. Again we see that the state of grains must be quite well described by only one parameter (perhaps local gas density).

6. Depletions are a function of z, the height above the plane of the Galaxy (50). Probably the extinction law also depends on z (83).

6.2 *Sites of Dust Formation*

Probably most dust is injected into the ISM from stars on the asymptotic giant branch, either C rich or O rich, although supernovae, despite a low *rate* of mass injection, might be important because of their large heavy-element composition. Carbon stars show an 11.15-μm feature of SiC with a quite uniform profile (26, 99). There is also a featureless optical/NIR continuum that can be modeled by amorphous carbon but not graphite (92, 106), unless the graphite is in small particles with a loose fractal structure (183). Oxygen-rich stars show the silicate feature with a profile that varies appreciably from star to star (99, 126). Differing physical conditions in the atmosphere affect the nature of the grains, and the silicate band in one star (2) shows clear signs of annealing. A few circumstellar shells show the 3.08-μm ice band as well.

The UV bump is found in C stars at 0.24 μm rather than at 0.2175 μm (67), and in one H-poor, C-rich planetary nebula (Abell 30) at 0.25 μm (63). These shifted wavelengths are consistent with amorphous C or fractal graphite grains. There is *no bump* in the circumstellar dust of oxygen-rich α Sco (153). The bump is seen in circumstellar dust surrounding a few hot stars (152) at the normal λ_{max}, but the dust might be interstellar, remaining from the epoch of the star's formation.

Novae and Wolf-Rayet stars (late-type WCs) are minor sources of dust because of their low mass input into the ISM (58a). Both presumably inject carbon-rich dust without silicates. Planetary nebulae represent a considerable source of the return of gas to the ISM (102) but are not a large source of dust because they have a low dust/gas ratio (131).

Isotopic anomalies in meteorites (see Section 6.3) prove that some dust forms in expanding supernova shells. Dust is also found within hot supernova remnants (48, 49), but it might have been produced by a presupernova red supergiant. How much dust is actually formed in supernovae is not known.

6.3 *Solar System Dust*

Primitive meteorites, interplanetary dust particles (IDPs), and cometary dust provide some information regarding interstellar grains, although all

solar system dust has been significantly processed, both chemically and physically, since having been in the pre–solar system molecular cloud. For reviews on the various types of objects, see (14, 15, 82).

Meteorites are almost entirely asteroidal in origin, since *cometary* meteoroids cannot survive entry into the Earth's atmosphere. Most meteorites have undergone obvious metamorphism, with carbonaceous chondrites being the most primitive. One of this class, the Murray meteorite, has tiny SiC inclusions showing isotopic anomalies (8, 186), proving an interstellar origin. The small amount of carbon in primitive meteorites is mostly poorly ordered, not graphitic, but tiny (ca. 25 Å) diamonds are present (97). It is difficult to imagine a solar system origin for the high temperatures and/or pressures needed to produce diamonds, so diamond bonding in interstellar carbon is strongly indicated. Meteoritic silicates are much more crystalline than the interstellar varieties, showing that meteorites must have been much warmer than interstellar temperatures. Graphite, if originally present, could have been lost by chemical reactions with water and hydrogen.

IDPs are both cometary and asteroidal in origin, with the cometary variety being more primitive and, therefore, relevant to interstellar dust. Some cometary IDPs, collected from high-flying aircraft, are a few microns in size, with a very fragile, open structure consisting of submicron mineral grains stuck together into an open matrix (see, e.g., 14, 15). Their silicates have been annealed to crystalline forms (143), with the types of minerals similar to those observed in cometary dust. Some of the carbon, poorly ordered but aromatic in nature, occurs as submicron grains. There is also carbon coated onto the silicate materials. Some IDPs have relatively large D/H ratios (185), suggestive of molecular clouds.

The crystalline structure of cometary silicates shows that even cometary dust has been fairly heavily modified from the original interstellar dust. There are whole particles consisting of volatile material containing C, H, O, and N ("CHON"), with little refractory material within; there are also low-density silicate and carbonaceous grains. Meteoroids (mostly cometary) entering the upper atmosphere have densities of 0.01–1 g cm^{-3}, so the fluffy refractory particles are common in comets and are probably present in interstellar dust, at least deep within molecular clouds.

In summary, solar system material shows that (*a*) small particles can survive all of the rigors of the ISM after formation in a supernova; (*b*) grains form large structures deep inside molecular clouds, with voids possibly packed with ices; and (*c*) heating and associated chemical processing took place before the formation of comets, possibly in the molecular cloud material.

7. EVOLUTION OF DUST

Relevant time scales show that the present form of interstellar dust must be more a reflection of the processing it has received within the ISM than a sample of the conditions at its origin. A typical parcel of gas and dust is cycled back and forth through molecular clouds several times during its lifetime, changing its grain properties significantly each time.

The lifetime of a grain against incorporation into stars can be estimated by dividing the surface density of the ISM by the rate of star formation. The local H I surface density is $\sim 10^7\ M_\odot\ \mathrm{kpc}^{-2}$ (89), and for H_2 is $3 \times 10^6\ M_\odot\ \mathrm{kpc}^{-2}$ (147). A mean rate of star formation of $3.4 \times 10^{-3}\ M_\odot\ \mathrm{kpc}^{-2}\ \mathrm{yr}^{-1}$ would account for the present surface density of low-mass ($M \leq M_\odot$) stars over 10^{10} yr (6); presumably the present rate is lower. High-mass stars contribute about $1.1 \times 10^{-3}\ M_\odot\ \mathrm{kpc}^{-2}\ \mathrm{yr}^{-1}$ (135). Therefore, the corresponding mean lifetime for a parcel of gas/dust in the ISM is more than 3 Gyr. On the other hand, about 30% of the local ISM is in molecular clouds, each with a lifetime of perhaps 10^8 yr (the time for the gas to proceed from one spiral arm to the next) or less. These numbers imply that a given parcel of gas has been into and out of a molecular cloud at least every 3×10^8 yr, or more than 10 times during its mean lifetime. Each time, the differences in extinction laws between diffuse dust and inner-cloud dust require that the grains be heavily modified.

Let us follow the state of a typical parcel of gas/dust near the Sun (see also 39). Since most of the mass of the local ISM is in H I, the parcel must spend the bulk of its time outside of molecular clouds. During this phase, about 10% of its mass is returned to the ISM from stars. Perhaps 10–20% of the returned gas is from hot stellar winds with no dust or from planetary nebulae with a dust/gas ratio lower than the ISM, providing substantial amounts of *gaseous* Fe, Al, and the other strongly depleted elements (81). Refractory elements must encounter grains frequently and stick to them very efficiently in order to achieve the observed strong depletions in the denser parts of the diffuse ISM.

Each time the gas/dust mixture is incorporated into the outer regions of a molecular cloud, many things happen to the grains: (*a*) The extinction law changes from diffuse dust to outer-cloud dust in such a way that the relative numbers of small, medium, and large grains depend primarily upon only one parameter (local gas density?), regardless of the local environment or past history. (*b*) The refractory elements are more strongly depleted onto the grains than in the diffuse phase. (*c*) The atomic H becomes molecular. Gaseous carbon recombines from C^+ to C^0 and finally to CO. (*d*) The grains almost certainly coagulate in the outer parts of molecular clouds before there is much coating of icy mantles. Much deeper

in the cloud, the fluffy micron-sized cometary and interplanetary dust particles can be produced by further coagulation of the silicate and carbonaceous parts of the grains, with ices probably filling the voids and producing the observed molecular absorption features. It is difficult to see how fluffy cometary mineral grains can form within the cloud if icy or organic refractory mantles envelop the minerals before the coagulation.

Coagulation seems to dominate the change in the size distribution in going from the diffuse ISM to outer-cloud dust. At least two well-observed stars in outer-cloud dust have $A(V)/N(\mathrm{H})$ smaller than in diffuse dust (CCM89). Since $\int [A(\lambda^{-1})/A(V)]\, d\lambda^{-1}$ is much lower in the outer-cloud dust than in diffuse dust (Figure 2), in these stars the integrated extinction per H atom is substantially smaller than in diffuse dust. This reduction in grain cross section per H atom, despite the accretion of small amounts of the refractory elements, can only be achieved by coagulation, which prevents the inner parts of the larger grains from participating efficiently in the extinction. Adding substantial coatings would increase, rather than reduce, the extinction cross section per H atom for the dust in the cloud.

There are real deviations of the various extinction laws about the mean. These differences must reflect somewhat different histories and present local environments (radiation fields, shocks, magnetic fields, etc) of the grains along each line of sight. Studying these deviations should lead to a better understanding of the factors influencing extinction laws.

8. SOME THEORIES, AND PROBLEMS WITH EACH

Space does not allow even a superficial discussion of all the many individual theories interpreting the observational evidence summarized above. Thus, we summarize a few.

1. *Bare silicate/graphite grains*: DL84, in a very careful discussion of the optical constants of both graphite and silicates, greatly extended in wavelength an older theory of Mathis, Rumpl & Nordsieck (114; often referred to as MRN). The features of the theory are that (*a*) individual grains are bare and homogeneous, composed of either silicate or graphite; (*b*) the size distribution is a power law, where $n(a)$, the number of grains of radius a, is proportional to $a^{-3.5}$; and (*c*) the size distribution is truncated at the upper end at 0.25 μm, with the lower end of sizes extending downward to a few angstroms to fit the *IRAS* data (41, 133), and very likely all the way to PAHs in order to produce the UIBs.

DL84 subjected their theory to a much more exacting comparison with observations than did most other authors. The fit to the extinction law for diffuse dust, over the entire observed wavelength range from 0.1 μm to

1000 μm, is impressively good. On the other hand, DL84 required that large graphite particles be produced from the amorphous carbon that late-type stars inject into the ISM. It is very difficult to understand how the necessary annealing can take place under interstellar conditions. Furthermore, the materials in the two types of grains (silicates and graphite) must be kept separate, despite the many cycles of coagulation and rearrangement of the size distributions that take place as the grains cycle into and out of clouds.

2. *Core/mantle grains*: Greenberg and his collaborators (see references in ref. 62) believe that the bulk of interstellar grains have refractory silicate cores covered with an organic refractory mantle. This mantle is produced from the processing by both UV photons and cosmic rays deep inside molecular clouds, after the icy mantles observed in such clouds are deposited upon the grain surfaces. Laboratory studies show that molecules in such mantles can be partially converted into free radicals that are chemically active enough to react violently when warmed, producing complex molecules (31). Such runaway reactions could be triggered on inner-cloud grains by cosmic rays. After such an event, an organic polymeric substance known as "organic refractory" material, stable at room temperatures remains. In this theory, organic refractory mantles on silicate cores produce the optical/NIR extinction, while the bump is produced by small graphite particles, PAHs produce the UIBs, and the shortest wavelength extinction is from small particles (probably silicates). Chlewicki & Laureijs (23) suggest that an additional component of iron will produce most of the 60-μm emission observed by *IRAS*.

These ideas have a great deal of appeal as regards events deep within clouds. The Greenberg scenario explains why interstellar molecules are found in the gas phase within dense clouds, where they should freeze onto grains in a short time—the runaway reactions drive off the molecules, and gas-phase chemistry takes place before refreezing onto grain surfaces. An alternative explanation for gas-phase molecules inside dense clouds is that a very rapid circulation of grains takes place between the surface and the center of the cloud (e.g. 21).

There are four problems as regards extending these ideas into diffuse dust: (*a*) Grains are larger in outer-cloud dust because of coagulation, not accretion of mantles, as shown by the reduced extinction per H atom in some cases. (*b*) Organic refractory mantles, which are less refractory than silicates and solid carbon, would be more readily destroyed by shocks in the diffuse ISM. The destruction rate of materials depends sensitively upon the binding energy (43, 44). (*c*) Solar system dust particles suggest that the silicate and carbon materials coagulate into large structures before icy mantles envelop them. (*d*) The 3.4-μm C–H absorption band, seen in

organic refractory material in the laboratory along with the 3.08-μm ice band, is locally weak or absent. The object with the strongest 3.4-μm band, IRS 7 near the galactic center (17), is not typical of local dust. The 3.08- and 3.4-μm bands are not yet seen toward the local star VI Cyg 12 (61) [for which $A(V) \approx 10$ mag], limiting these bands to less than 0.3 the strength, per $A(V)$, of those for IRS 7. The 3.4-μm band is seen in Lynga 8/IRS 3 [154; $A(V) = 17$], about 0.4 times as strong as for IRS 7. The 3.4-μm band is always accompanied by a stronger 3.08-μm ice feature, and there are some lines of sight (64) with no ice band for $A(V) < 20$ mag.

It is possible (156) that the organic refractory mantles are so heavily processed that they lose almost all of their N and O, becoming essentially amorphous carbon. This material would be difficult to distinguish from amorphous C injected directly into the ISM from carbon stars. In this case, the Greenberg theory is very similar to composite-grain theories (see below).

3. *Silicate cores with amorphous carbon mantles*: Duley et al (47) suggest that grains are silicates with mantles of hydrogenated amorphous carbon (HAC). One population is very small and produces the bump by $(OH)^-$ ion absorption in the presence of Si atoms. (All other theories produce the bump from well-ordered carbon.) The UIBs are caused by absorption of UV photons by "islands" of HAC on the silicate core surfaces, so thermally isolated that they can radiate like free particles [for about 1 second! (133)]. The rapid increase of extinction with wave number for $\lambda^{-1} > 6$ μm^{-1} is produced by diamondlike bonding in the "amorphous" C.

This theory makes several predictions that can be tested. It explains the differences between diffuse dust and outer-cloud dust rather naturally as arising from different depletions of carbon onto the silicate cores. However, it requires a very large fraction of the Si atoms to have OH^- ions nearby, near the surfaces of small grains, even if the bump transition in OH^- has an oscillator strength of unity. The thermal isolation of the "islands" of HAC is difficult to achieve.

4. *Composite grains*: Mathis & Whiffen (113) and Tielens (156) suggest that interstellar grains consist of an assembly of small particles of carbon and silicates, jumbled together loosely. These grains are the natural result of coagulation and disruption of grains as they cycle into clouds. The particles inside the porous structure are protected from shocks and might well be covered with highly processed organic material. The bump is provided by small graphitic particles; PAHs can produce the UIBs. The rise in extinction for $\lambda < 0.16$ μm is provided by the diamond bonding in "amorphous" C. The composite grains are mostly open, in analogy with interplanetary dust particles. However, too much porosity provides too large an opacity in the FIR, making the grains too cold because they

radiate efficiently. It is difficult to calculate the extinction of composite grains, so the calculated fit should be taken as provisional.

5. *Fractal grains*: Wright (182) suggested that interstellar grains are the product of coagulation into very large fractal structures resembling twisted branches (65). If one defines the fractal dimension α by $M \propto R^{\alpha}$, then α depends upon the sequence of coagulation (and the probability of the fractal grains' breaking up, which is neglected in the calculations). In general $\alpha < 3$, and in some cases $\alpha < 2$. One of the major features of fractal grains is a FIR absorption per unit mass larger by an order of magnitude or more than that for solid grains.

Fractal grains can explain very large radar backscattering in comets (183) without large masses of dust. They also explain the very shallow (λ^{-1}) wavelength dependence of the submillimeter opacity observed in some very dense nebulae (Section 3.2.3). However, the FIR opacity of fractal grains is so large that the grains would be too cold to explain the observed FIR spectrum of galactic dust ($T \approx 20$ K).

6. *Biological grains*: Hoyle, N. C. Wickramasinghe, and others (76, 161, and references therein) have suggested that the grains producing visual extinction have a biological origin, with the bump provided by graphite. The extinction and polarization laws are fitted reasonably well. However, there are two problems with the model: (*a*) There is not enough cosmic phosphorus to accommodate the amount found in organisms (45, 164; but see 74). The cosmic abundance of P is low, and most of it is in the gas phase for low-density lines of sight, so this criticism seems valid. (*b*) Organisms, even when dried, show strong O–H and C–H stretch absorptions (75), which are not seen except deep within molecular clouds.

9. SUMMARY

"Interstellar dust" refers to materials with rather different properties, and the "mean extinction law" of Seaton (149) or Savage & Mathis (144) should be replaced by the expression given in CCM89, using the appropriate value of total-to-selective extinction R_V. The older laws were appropriate for the diffuse ISM, but dust in clouds differs dramatically in its extinction law (Figure 2). However, there are certainly real deviations from the mean extinction law (see error bars in the inset in Figure 2). The extinction law for $\lambda > 0.9$ μm seems to be independent of environment, to within the present observational errors. Other diagnostics of dust, especially the depletions from the gas phase, confirm that properties of the grains vary along different lines of sight, but only one parameter, probably related to the local gas density, determines the grain properties surprisingly well.

Dust is heavily processed while in the ISM by being included within

clouds and cycled back into the diffuse ISM many times during its lifetime. Consequently, grains probably reflect only a trace of their origin, although meteoritic inclusions with isotopic anomalies prove that some tiny particles survive intact from a supernova origin to the present. Grains apparently grow by coagulation while in clouds. Cometary and interplanetary dust suggests that very large sized grains are produced before extensive icy mantles are formed. Within the dark clouds, there is likely processing of the icy mantles by cosmic rays or by the UV radiation produced by cosmic rays, and heavy molecules are released by runaway reactions. If there is an organic refractory mantle remaining after this processing, it is probably converted to almost pure amorphous carbon by the continued processing to which the grains are subjected.

There are several theories that explain the extinction law for diffuse dust, but a much more challenging problem is to understand the relation between dust of all types. The evolution of dust is probably the next theoretical challenge.

ACKNOWLEDGMENTS

This review has been partially supported by contract 957996 with the Jet Propulsion Laboratory and grant NAGW-1768 with NASA. Comments and assistance from L. J. Allamandola, J. A. Cardelli, G. C. Clayton, B. T. Draine, P. G. Martin, and B. D. Savage are appreciated.

Literature Cited

1. Aitken, D. K., Bailey, J. E., Roche, P. F., Hough, J. H. 1985. *MNRAS* 215: 815
2. Aitken, D. K., Roche, P. F., Smith, C. H., James, S. D., Hough, J. H. 1988. *MNRAS* 230: 629
3. Allamandola, L. J., Tielens, A. G. G. M., eds. 1989. *Interstellar Dust, IAU Symp. No. 135*. Dordrecht: Kluwer. 530 pp.
4. Allamandola, L. J., Tielens, A. G. G. M., Barker, J. R. 1989. *Ap. J. Suppl.* 71: 733
5. Ardeberg, A., Virdefors, B. 1982. *Astron. Astrophys.* 115: 347
6. Bahcall, J. N., Soneira, R. M. 1980. *Ap. J. Suppl.* 44: 73
7. Bailey, M. E., Williams, D. A., eds. 1988. *Dust in the Universe*. Cambridge: Univ. Press. 573 pp.
8. Bernatowicz, T., Fraundorf, G., Tang, M., Anders, E., Wopenka, B., et al. 1987. *Nature* 330: 728
9. Bohlin, R. C., Savage, B. D., Drake, J. F. 1978. *Ap. J.* 224: 132
9a. Bohren, C. E., Huffman, D. R. 1983. *Absorption and Scattering of Light by Small Particles*. New York: Wiley. 530 pp.
10. Borghesi, A., Bussoletti, E., Colangeli, L. 1987. *Ap. J.* 314: 422
11. Bouchet, P., Lequeux, J., Maurice, E., Prévot, L., Prévot-Burnichon, M. L. 1985. *Astron. Astrophys.* 149: 330
12. Boulanger, F., Pérault, M. 1988. *Ap. J.* 330: 964
13. Boulanger, F., Beichman, C., Désert, F. X., Helou, G., Pérault, M., Ryter, C. 1988. *Ap. J.* 332: 328
14. Brownlee, D. E. 1985. *Annu. Rev. Earth Planet. Sci.* 13: 147
15. Brownlee, D. E. 1989. In *Highlights of Astronomy*, ed. D. McNally, 8: 281. Dordrecht: Kluwer
16. Butchart, I., Whittet, D. C. B. 1983. *MNRAS* 202: 971
17. Butchart, I., McFadzean, A. D., Whittet, D. C. B., Geballe, T. R., Greenberg, J. M. 1986. *Astron. Astrophys.* 154: L5

18. Cardelli, J. A., Savage, B. D. 1988. *Ap. J.* 325: 864
19. Cardelli, J. A., Clayton, G. C., Mathis, J. S. 1988. *Ap. J. Lett.* 329: L33
20. Cardelli, J. A., Clayton, G. C., Mathis, J. S. 1989. *Ap. J.* 345: 245 (CCM89)
21. Chièze, J. P., Pineau des Forêts, G. 1989. *Astron. Astrophys.* 221: 89
22. Chini, R., Krügel, E., Kreysa, E. 1989. *Astron. Astrophys.* 216: L5
23. Chlewicki, G., Laureijs, R. J. 1988. *Astron. Astrophys.* 207: L11
24. Clayton, G. C., Martin, P. G. 1985. *Ap. J.* 288: 558
25. Clayton, G. C., Mathis, J. S. 1988. *Ap. J.* 327: 911
26. Cohen, M. 1984. *MNRAS* 206: 137
27. Cohen, M., Allamandola, L. J., Tielens, A. G. G. M., Bregman, J., Simpson, J., et al 1986. *Ap. J.* 302: 737
28. Cohen, M., Tielens, A. G. G. M., Bregman, J. D. 1989. *Ap. J. Lett.* 344: L13
29. Cohen, M., Tielens, A. G. G. M., Bregman, J., Witteborn, F. C., Rank, D. M., et al. 1989. *Ap. J.* 341: 246
30. Cox, P., Mezger, P. G. 1989. *Astron. Astrophys. Rev.* 1: 49
31. d'Hendecourt, L. B., Allamandola, L. J., Grim, R. J. A., Greenberg, J. M. 1986. *Astron. Astrophys.* 158: 119
32. d'Hendecourt, L. B., Léger, A., Olofsson, G., Schmidt, W. 1986. *Astron. Astrophys.* 170: 91
33. Day, K. L. 1979. *Ap. J.* 234: 158
34. Désert, F. X., Boulanger, F., Shore, S. N. 1986. *Astron. Astrophys.* 160: 295
35. Dragovan, M. 1986. *Ap. J.* 308: 270
36. Draine, B. T. 1988. *Ap. J.* 333: 848
37. Draine, B. T. 1989. In *Infrared Spectroscopy in Astronomy. Proc. ESLAB Symp., 22nd.* In press
38. Draine, B. T. 1989. See Ref. 3, p. 313
39. Draine, B. T. 1990. In *The Evolution of the Interstellar Medium*, ed. L. Blitz. San Francisco: Astron. Soc. Pac. Press. In press
40. Draine, B. T. 1990. In *The Interstellar Medium in Galaxies*, ed. H. A. Thronson, J. M. Shull. Dordrecht: Kluwer. In press
41. Draine, B. T., Anderson, N. 1985. *Ap. J.* 292: 494
42. Draine, B. T., Lee, H. M. 1984. *Ap. J.* 285: 89 (DL84)
43. Draine, B. T., Salpeter, E. E. 1979. *Ap. J.* 231: 77
44. Draine, B. T., Salpeter, E. E. 1979. *Ap. J.* 231: 438
45. Duley, W. W. 1984. *Q. J. R. Astron. Soc.* 25: 109
46. Duley, W. W. 1985. *MNRAS* 215: 259
47. Duley, W. W., Jones, A. P., Williams, D. A. 1989. *MNRAS* 236: 709
48. Dwek, E., Dinerstein, H. L., Gillett, F. C., Hauser, M. G., Rice, W. L. 1987. *Ap. J.* 315: 571
49. Dwek, E., Petre, R., Szymkowiak, A., Rice, W. L. 1987. *Ap. J. Lett.* 320: L27
50. Edgar, R. J., Savage, B. D. 1989. *Ap. J.* 340: 762
51. FitzGerald, M. P. 1968. *Astron. J.* 73: 983
52. FitzGerald, M. P., Stephens, T. C., Witt, A. N. 1976. *Ap. J.* 208: 709
53. Fitzpatrick, E. L. 1985. *Ap. J.* 299: 219
54. Fitzpatrick, E. L., Massa, D. 1986. *Ap. J.* 307: 286 (FM86)
55. Fitzpatrick, E. L., Massa, D. 1988. *Ap. J.* 328: 734
56. Gatley, I., Hasegawa, T., Suzuki, H., Garden, R., Brand, P. W. J. L., et al. 1987. *Ap. J. Lett.* 318: L73
57. Geballe, T. R., Tielens, A. G. G. M., Allamandola, L. J., Moorhouse, A., Brand, P. W. J. L. 1989. *Ap. J.* 341: 278
58. Gehrels, T. 1974. *Astron. J.* 79: 590

58a. Gehrz, R. 1989. See Ref. 3, p. 445

59. Giard, M., Pajot, F., Lamarre, J. M., Serra, G., Caux, E. 1989. *Astron. Astrophys.* 215: 92
60. Gillett, F. C., Forrest, W. J., Merrill, K. M., Capps, R. W., Soifer, B. T. 1975. *Ap. J.* 200: 609
61. Gillett, F. C., Jones, T. W., Merrill, K. M., Stein, W. A. 1975. *Astron. Astrophys.* 45: 77
62. Greenberg, J. M. 1989. In *Highlights of Astronomy*, ed. D. McNally, 8: 241. Dordrecht: Kluwer
63. Greenstein, J. L. 1981. *Ap. J.* 245: 124
64. Harris, D. H., Woolf, N. J., Rieke, G. H. 1978. *Ap. J.* 226: 829
65. Hawkins, I., Wright, E. L. 1988. *Ap. J.* 324: 46
66. Hecht, J. H. 1987. *Ap. J.* 314: 429
67. Hecht, J. H., Holm, A. V., Donn, B., Wu, C.-C. 1984. *Ap. J.* 280: 228
68. Hecht, J. H., Russell, R. W., Stephens, J. R., Grieve, P. R. 1986. *Ap. J.* 309: 90
69. Henyey, L. G., Greenstein, J. L. 1941. *Ap. J.* 93: 70
70. Hildebrand, R. H. 1983. *Q. J. R. Astron. Soc.* 24: 267
71. Hildebrand, R. H. 1988. *Q. J. R. Astron. Soc.* 29: 327
72. Hildebrand, R. H., Dragovan, M., Novak, G. 1984. *Ap. J. Lett.* 284: L51
73. Hobbs, L. M., York, D. G., Oegerle, W. 1982. *Ap. J. Lett.* 252: L21

73a. Hollenbach, D. J., Thronson, H. A. Jr. 1987. *Interstellar Processes. Astrophys. Space Sci. Libr.*, Vol. 134. Dordrecht: Reidel

74. Hoyle, F., Wickramasinghe, N. C. 1984. *Astrophys. Space Sci.* 103: 189
75. Hoyle, F., Wickramasinghe, N. C., Al-

Mufti, S., Olavesen, A. H., Wickramasinghe, D. T. 1982. *Astrophys. Space Sci.* 83: 405
76. Jabbir, N. L., Jabbar, S. R., Salih, A. H., Majeed, Q. S. 1986. *Astrophys. Space Sci.* 123: 351
77. Jakobsen, P., Bowyer, S., Kimble, R., Jelinsky, P., Grewing, M., et al. 1984. *Astron. Astrophys.* 139: 481
78. Jenkins, E. B. 1987. See Ref. 73a, p. 533
79. Jones, T. J., Hyland, H. 1980. *MNRAS* 192: 354
80. Joseph, C. L. 1988. *Ap. J.* 335: 157
81. Jura, M. 1987. See Ref. 73a, p. 3
82. Kerridge, J. F., Mathews, M. S., eds. 1988. *Meteorites and the Early Solar System.* Tucson: Univ. Ariz. Press
83. Kiszkurno-Koziej, E., Lequeux, J. 1987. *Astron. Astrophys.* 185: 291
84. Knacke, R. F., Capps, R. W. 1979. *Astron. J.* 84: 1705
85. Knacke, R. F., Krätchmer, W. 1980. *Astron. Astrophys.* 80: 281
86. Koornneef, J. 1982. *Astron. Astrophys.* 107: 247
87. Koornneef, J. 1983. *Astron. Astrophys.* 128: 84
88. Krätchmer, W., Huffman, D. R. 1979. *Astrophys. Space Sci.* 61: 195
89. Kulkarni, S. R., Heiles, C. 1987. See Ref. 73a, p. 87
90. Laureijs, R. J., Mattila, K., Schnur, G. 1987. *Astron. Astrophys.* 184: 269
91. Laureijs, R. J., Chlewicki, G., Clark, F. O. 1988. *Astron. Astrophys.* 192: L13
92. Le Bertre, T. 1987. *Astron. Astrophys.* 176: 107
93. Lee, H. M., Draine, B. T. 1985. *Ap. J.* 290: 211
94. Léger, A., d'Hendecourt, L., Défourneau, D. 1989. *Astron. Astrophys.* 216: 148
95. Lenzen, R., Hodapp, K.-W., Solf, J. 1984. *Astron. Astrophys.* 137: 202
96. Lequeux, J., Maurice, E., Prévot-Burnichon, M. L., Prévot, L., Rocca-Volmerange, B. 1982. *Astron. Astrophys.* 113: L15
97. Lewis, R. S., Tang, M., Wacker, J. F., Anders, E., Steel, E. 1987. *Nature* 326: 160
98. Lillie, C. F., Witt, A. N. 1976. *Ap. J.* 208: 64
99. Little-Marenin, I. R. 1986. *Ap. J. Lett.* 307: L15
100. Lockman, F. J., Jahoda, K., McCammon, D. 1986. *Ap. J.* 302: 432
101. Lucke, P. B. 1978. *Astron. Astrophys.* 64: 367
102. Maciel, W. J. 1981. *Astron. Astrophys.* 98: 406
103. Martin, C., Bowyer, S. 1989. *Ap. J.* 338: 677
104. Martin, N., Maurice, E., Lequeux, J. 1989. *Astron. Astrophys.* 215: 219
105. Martin, P. G. 1975. *Ap. J.* 202: 393
106. Martin, P. G., Rogers, C. 1987. *Ap. J.* 322: 374
107. Martin, P. G., Rouleau, F. 1989. *Berkeley EUV Colloq.*
108. Martin, P. G., Whittet, D. C. B. 1990. *Ap. J.* Submitted for publication
109. Massa, D., Fitzpatrick, E. L. 1986. *Ap. J. Suppl.* 60: 305
110. Mathis, J. S. 1973. *Ap. J.* 173: 815
111. Mathis, J. S. 1986. *Ap. J.* 308: 281
112. Mathis, J. S. 1986. *Publ. Astron. Soc. Pac.* 98: 995
113. Mathis, J. S., Whiffen, G. 1989. *Ap. J.* 341: 808
114. Mathis, J. S., Rumpl, W., Nordsieck, K. H. 1977. *Ap. J.* 217: 425
115. Matsumoto, T., Hayakawa, S., Matsuo, H., Murakami, H., Sato, S., et al. 1988. *Ap. J.* 329: 567
116. Mattila, K. 1979. *Astron. Astrophys.* 78: 253
117. Mauche, C. W., Gorenstein, P. 1986. *Ap. J.* 302: 371
118. McCarthy, J. F., Forrest, W. J., Briotta, D. A., Houck, J. R. 1980. *Ap. J.* 242: 965
119. Morgan, D. H., Nandy, K. 1982. *MNRAS* 199: 979
120. Murthy, J., Henry, R. C., Feldman, P. D., Tennyson, P. D. 1988. *Ap. J.* 336: 954
121. Nandy, K., Morgan, D. H., Willis, A. J., Wilson, R., Gondhalekar, P. M. 1981. *MNRAS* 196: 955
122. Neckel, Th., Klare, G. 1980. *Astron. Astrophys. Suppl.* 42: 251
123. Nuth, J. A. III, Stencel, R. E., eds. 1986. *Interrelationships Among Circumstellar, Interstellar, and Interplanetary Dust. NASA Conf. Publ. 2403.* Washington, DC: US Gov. Print. Off.
124. Pajot, F., Gispert, R., Lamarre, J. M., Pomerantz, M. A., Puget, J. L., Serra, G. 1989. *Astron. Astrophys.* 224: 107
125. Papoular, R., Conard, J., Giuliano, M., Kister, J., Mille, G. 1989. *Astron. Astrophys.* 217: 204
126. Papoular, R., Pegourie, B. 1983. *Astron. Astrophys.* 128: 335
127. Paresce, F., McKee, C., Bowyer, S. 1980. *Ap. J.* 240: 387
128. Pegourie, B., Papoular, R. 1985. *Astron. Astrophys.* 142: 451
129. Pendleton, Y., Tielens, A. G. G. M., Werner, M. 1990. *Ap. J.* In press
130. Pendleton, Y., Werner, M., Capps, R., Lester, D. 1986. *Ap. J.* 311: 360
131. Pottasch, S. R., Baud, B., Beitema, D., Emerson, J., Habing, H. J., et al. 1984. *Astron. Astrophys.* 138: 10

132. Price, S. D. 1981. *Astron. J.* 86: 193
133. Puget, J. L., Léger, A. 1989. *Annu. Rev. Astron. Astrophys.* 27: 161
134. Purcell, E. M. 1979. *Ap. J.* 231: 404
135. Ratnatunga, K. U., van den Bergh, S. 1989. *Ap. J.* 343: 713
136. Rieke, G. H., Lebofsky, M. J. 1985. *Ap. J.* 288: 618
137. Roche, P. F., Aitken, D. K. 1984. *MNRAS* 208: 481
138. Roche, P. F., Aitken, D. K. 1985. *MNRAS* 215: 425
139. Rush, W. F., Witt, A. N. 1975. *Astron. J.* 80: 31
140. Russell, R. W., Soifer, B. T., Willner, S. P. 1978. *Ap. J.* 220: 568
141. Ryter, C., Puget, J. L., Pérault, M. 1987. *Astron. Astrophys.* 186: 312
142. Sakata, A., Wada, S., Tanabe, T., Onaka, T. 1984. *Ap. J. Lett.* 287: L51
143. Sandford, S. A., Walker, R. M. 1985. *Ap. J.* 291: 838
144. Savage, B. D., Mathis, J. S. 1979. *Annu. Rev. Astron. Astrophys.* 17: 73
145. Schloerb, F. P., Snell, R. L., Schwartz, P. R. 1987. *Ap. J.* 319: 426
146. Schmidt, G. D., Cohen, M., Margon, B. 1980. *Ap. J. Lett.* 239: L133
147. Scoville, N. Z., Sanders, D. B. 1987. See Ref. 73a, p. 21
148. Seab, C. G., Snow, T. P. 1985. *Ap. J.* 295: 485
149. Seaton, M. J. 1979. *MNRAS* 187: 73P
150. Sellgren, K. 1984. *Ap. J.* 277: 623
151. Sellgren, K., Allamandola, L. J., Bregman, J. D., Werner, M. W., Wooden, D. H. 1985. *Ap. J.* 299: 416
151a. Serkowski, K., Mathewson, D. S., Ford, V. L. 1975. *Ap. J.* 196: 261
152. Sitko, M. L., Savage, B. D., Meade, M. R. 1981. *Ap. J.* 246: 161
153. Snow, T. P., Buss, R. H., Gilra, D. P., Swing, J.-P. 1987. *Ap. J.* 321: 921
154. Tapia, M., Persi, P., Roth, M., Ferrari-Toniolo, M. 1989. *Astron. Astrophys.* 225: 488
155. Tennyson, P. D., Henry, R. C., Feldman, P. D., Hartig, G. F. 1988. *Ap. J.* 330: 435
156. Tielens, A. G. G. M. 1989. See Ref. 3, p. 239
157. Tielens, A. G. G. M., Allamandola, L. J. 1987. See Ref. 73a, p. 397
158. Toller, G. N. 1981. PhD thesis. State Univ. N.Y., Stony Brook
159. Vrba, F. J., Rydgren, A. E. 1985. *Astron. J.* 90: 1490
160. Volk, K., Kwok, S. 1988. *Ap. J.* 331: 435
161. Wallis, M. K., Wickramasinghe, N. C., Hoyle, F., Rabilizirov, R. 1989. *MNRAS* 238: 1165
162. Weintraub, D., Sandell, G., Duncan, W. D. 1989. *Ap. J. Lett.* 340: L69
163. Werner, M. W., Davidson, J. A., Hildebrand, R. H., Morris, M. R., Novak, G., Platt, S. R. 1988. *Ap. J.* 333: 729
164. Whittet, D. C. B. 1984. *MNRAS* 210: 479
165. Whittet, D. C. B. 1987. *Q. J. R. Astron. Soc.* 28: 303
166. Whittet, D. C. B. 1988. See Ref. 7, p. 25
167. Whittet, D. C. B., van Breda, I. G. 1978. *Astron. Astrophys.* 66: 57
168. Whittet, D. C. B., van Breda, I. G. 1980. *MNRAS* 192: 467
169. Whittet, D. C. B., Bode, M. F., Longmore, A. J., Adamson, A. J., McFadzean, A. D., et al. 1988. *MNRAS* 233: 321
170. Wilking, B. A., Lebofsky, M. J., Rieke, G. H. 1982. *Astron. J.* 87: 695
171. Willner, S. P. 1984. In *Galactic and Extragalactic Infrared Spectroscopy*, ed. M. F. Kessler, J. P. Phillips, p. 37. Dordrecht: Reidel
172. Willner, S. P., Gillett, F. C., Herter, T. L., Jones, B., Krassner, J., et al. 1982. *Ap. J.* 253: 174
173. Witt, A. N. 1968. *Ap. J.* 152: 59
174. Witt, A. N. 1988. See Ref. 3, p. 1
175. Witt, A. N., Schild, R. E. 1988. *Ap. J.* 325: 837
176. Witt, A. N., Bohlin, R. C., Stecher, T. P. 1984. *Ap. J.* 279: 698
177. Witt, A. N., Bohlin, R. C., Stecher, T. P. 1986. *Ap. J. Lett.* 305: L23
178. Witt, A. N., Schild, R. E., Kraiman, J. B. 1984. *Ap. J.* 262: 708
179. Witt, A. N., Stecher, T. P., Boroson, T. A., Bohlin, R. C. 1989. *Ap. J. Lett.* 336: L21
180. Witteborn, F. C., Sandford, S. A., Bregman, J. D., Allamandola, L. J., Cohen, M., et al. 1989. *Ap. J.* 341: 270
181. Woody, D. P., Scott, S. L., Scoville, N. Z., Mundy, L. G., Sargent, A. I., et al. 1989. *Ap. J. Lett.* 337: L41
182. Wright, E. L. 1987. *Ap. J.* 320: 818
183. Wright, E. L. 1989. *Ap. J. Lett.* 346: L89
184. York, D., Drake, J., Jenkins, E., Morton, D., Rogerson, J., Spitzer, L. 1973. *Ap. J. Lett.* 182: L1
185. Zinner, E., McKeegan, K. D., Walker, R. M. 1983. *Nature* 305: 119
186. Zinner, E., Tang, M., Anders, E. 1987. *Nature* 330: 730